ASM-FDTD Combine the Prony's Method to Simulate the EMP Propagation in Tunnel

Yun-Fei Mao, Hong-Bing Wu, Jia-Hong Chen, and Xu-Wei Su

China Satellite Maritime Tracking and Control Department
Jiangyin, 2144000, China
myf4494@163.com, hongbing@163.com, stone_cjh@sina.com, suxuwei1983@163.com

Abstract ─ The aliasing problem in ASM-FDTD is presented in detail, to overcome the problem of the ASM-FDTD method to simulate the Electromagnetic pulse (EMP) propagation in periodic tunnel structure, the prony's method is employed to model the time domain field of the ASM-FDTD. The solution of the aliasing problem is achieved through evaluating of the exponential models at intermediate spectral points with interpolation, and the computational resource is also saved for the later time response. The accuracy of the approach is verified by comparing the results with the MW-FDTD which is calculated by parallel computing.

Index Terms ─ Aliasing problem, array scanning method (ASM), finite-difference time domain (FDTD), periodic structures, tunnel.

I. INTRODUCTION

EMP propagation in tunnel is a significant subject to study, the interest mainly comes from two aspects. First is the electromagnetic protection against the EMP weapons, second is the ultra-wideband (UWB) communication in tunnel. The well-known finite-different time-domain (FDTD) technique is an ideal method due to its accuracy and flexibility, but the main problem is the high memory requirement and heavy computational burden when deal with these large-scale problems [1]-[12]. A successful technique to deal with this problem is MW-FDTD [13] which requires a relatively small FDTD computational mesh along with the pulse, this technique is applicable only when the significant pulse energy exists over a small part of the propagation path at any instant time. However, when a long distance is simulated, much computer resources are required. The ASM-FDTD [14]-[16] method is a novel technique, combining the spectral FDTD method [17] to model the excitation of infinite periodic structures. Tunnel system is periodic in one dimension. By considering the influence of the steel-bar structure in the around reinforce concrete, and the impressed excitation sources is often introduced at the sectional surfaces. So the ASM-FDTD technique can be dealt with, as a result, only a single periodic cell of the periodic tunnel structure needs to be considered. The computational resources are reduced.

However, in the implementation of the ASM-FDTD technique, it involves the aliasing problems which is similar to the Discrete Fourier Transform (DFT). And it is difficult to distinguish the overlapping signals. To overcome the problem, it needs to increase the number of spectral sampling points in Brillouin zone or to enlarge the size of periodic cell, which requires a lot of computational resources. Another problem is a long time running is needed when simulating the long distant tunnel structure.

The Prony's method [18] is a technique to model the sampled data as a linear superposition of complex exponentials. In the present paper, the Prony's method is combined with the ASM-FDTD method, by using the periodic sources with different phase shift. Results show that they are agree very well with each other, which means the laws of the integral field could be expressed by a set of exponential parameter values simply. Firstly we obtain the exponential parameter values from a short time-domain response of the integral field with respect to every spectral points, then the exponential models is used to extrapolate the later time response of the integral field, so a large computation time will be reduced. On the other hand, based on the known parameter values corresponding to the finite spectral sampled points, we could estimate the parameter values at every spectral point in Brillouin zone approximately, by using interpolation method. Thus the integral fields at every spectral point are also obtained by the exponential models analytically and the aliasing problem can be solved.

This paper is organized as follows. In Section II, the Fourier transform (FT) property of the ASM-FDTD is presented, the details of the aliasing problem is made clear systematically according to the FT theory. In Section III we outline the application of Prony's method to fit the exponential model to the integral field and show the exponential parameter values versus the spectral sampling points. In Section IV, the estimation

Submitted On: March 19, 2019
Accepted On: November 17, 2019

of the parameter values by interpolation and the solution to the aliasing problem are described. The final results of the problem are compared with the MW-FDTD method.

II. FOURIER TRANSFORM PROPERTY OF ASM

In time domain, $E_{tot}^{\infty}(r,r_0,k_z,t)$ is the total electric field at r in the infinite periodic structure along the z direction produced by a set of sources at $r_0+m\alpha \mathrm{l}_z (m=0,\pm 1...)$ with a phase shift $\exp(-jk_z\alpha)$. Between the adjacent sources and $E_{tot}(r,r_0+n\alpha \mathrm{l}_z,k_z,t)$ is the field at r in the same periodic environment produced by a single source at $r_0+n\alpha \mathrm{l}_z$, according to the superposition principle we can obtain:

$$\begin{aligned} E_{tot}^{\infty}(r,r_0,k_z,t) &= \sum_{n=-\infty}^{\infty} E_{tot}(r,r_0+n\alpha \mathrm{l}_z,k_z,t) \\ &= \sum_{n=-\infty}^{\infty} E_{tot}(r,r_0+n\alpha \mathrm{l}_z,t)e^{-jk_z n\alpha} \end{aligned}, \quad (1)$$

where α is the period along the z direction and k_z is the phasing parameter. Multiply both side of (1) with $e^{-jk_z m\alpha}$ and integrate from π/α to $-\pi/\alpha$ with k_z, following the orthogonal property of the complex exponential function we have:

$$E_{tot}(r,r_0-m\alpha 1_z,t)=\frac{\alpha}{2\pi}\int_{-\pi/\alpha}^{\pi/\alpha} E_{tot}^{\infty}(r,r_0,k_z,t)e^{-jk_z m\alpha}dk_z . \quad (2)$$

In an infinite periodic structure,

$$E_{tot}(r,r_0-m\alpha 1_z,t)=E_{tot}(r+m\alpha 1_z,r_0,t). \quad (3)$$

Substitute (3) into (2),

$$E_{tot}(r+m\alpha 1_z,r_0,t)=\frac{\alpha}{2\pi}\int_{-\pi/\alpha}^{\pi/\alpha} E_{tot}^{\infty}(r,r_0,k_z,t)e^{-jk_z m\alpha}dk_z . \quad (4)$$

So $E_{tot}(r+m\alpha \mathrm{l}_z,r_0,t)$ at $r_0+m\alpha \mathrm{l}_z$ produced by a single source at r in $n=0$ periodic cell can be calculated by $E_{tot}^{\infty}(r,r_0,k_z,t)$ which could be obtained by spectral FDTD with the periodic condition:

$$E_{tot}^{\infty}(r+\alpha 1_z,r_0,k_z,t)=E_{tot}^{\infty}(r,r_0,k_z,t)e^{-jk_z\alpha}. \quad (5)$$

From (1) we can find that $E_{tot}^{\infty}(r,r_0,k_z,t)$ is periodic with period $2\pi/\alpha$:

$$E_{tot}^{\infty}(r,r_0,k_z+i\frac{2\pi}{\alpha},t)=E_{tot}^{\infty}(r,r_0,k_z,t),\ i=0,1..., \quad (6)$$

the property of conjugation,

$$E_{tot}^{\infty}(r,r_0,-k_z,t)=E_{tot}^{\infty}(r,r_0,k_z,t)^{*}. \quad (7)$$

For brevity we set:

$$\alpha=f_0, T_0=1/f_0, k_z=2\pi\tau, \quad (8)$$

$$E_{tot}(r+n\alpha \mathrm{l}_z,r_0,t)=G(nf_0),\ E_{tot}^{\infty}(r,r_0,k_z,t)=g(\tau). \quad (9)$$

Substitute them into (4) and (6):

$$G(nf_0)=\frac{1}{T_0}\int_{-T_0/2}^{T_0/2} g(\tau)e^{-j2\pi nf_0\tau}d\tau , \quad (10)$$

$$g(\tau+iT_0)=g(\tau)\quad (i=0,\pm 1,\cdots). \quad (11)$$

By using the simple left endpoint rule of numerical integration, from (10) we have:

$$G_d(nf_0)=\frac{1}{N}\sum_{k=-N/2}^{N/2-1} g(kT)e^{-j2\pi nk/N}, \quad (12)$$

where $T=T_0/N$ is the sampling interval and N is the number of sampling points, substitute (8) and (9) into (12):

$$E_{tot}(r+n\alpha \mathrm{l}_z,r_0,t)=\frac{1}{N}\sum_{k=-N/2}^{N/2-1} E_{tot}^{\infty}(r,r_0,\frac{k}{N\alpha},t)e^{-j2\pi nk/N}. \quad (13)$$

For the property of (7) that only half of the sampling points need to be computed here.

Suppose that $h(\tau)$ is the sampling function and its Fourier transform (FT) is $H(f)$, which can be shown:

$$h(\tau)=\sum_{k=-\infty}^{\infty}\delta(\tau-kT)\Leftrightarrow H(f)=\frac{1}{T}\sum_{k=-\infty}^{\infty}\delta(f-\frac{k}{T}), \quad (14)$$

$g(\tau)$ is a periodic continuous function, its FT is $G(f)$ can be expressed as:

$$G(f)=\sum_{n=-\infty}^{\infty} G(nf_0)\delta(f-nf_0). \quad (15)$$

Sample $g(\tau)$ with $h(\tau)$, the result is $g(\tau)h(\tau)$ and its FT can be expressed as [19]:

$$GH(f)=\sum_{n=-\infty}^{\infty} a_n\delta(f-nf_0), \quad (16)$$

$$\begin{aligned} a_n &= \frac{1}{T_0}\sum_{k=-N/2}^{N/2-1} g(kT)e^{-j2\pi nk/N} \\ &= \frac{G_d(nf_0)}{T} \end{aligned}. \quad (17)$$

According to the convolution theorem, from (14) and (15) we have:

$$\begin{aligned} GH(f) &= \sum_{n=-\infty}^{\infty} G(nf_0)\delta(f-nf_0)*H(f) \\ &= \sum_{m=-\infty}^{\infty}\left[\sum_{n=-\infty}^{\infty}\frac{1}{T}G(nf_0)\delta(f-nf_0-mNf_0)\right] \end{aligned}. \quad (18)$$

Form (16) and (18) we get:

$$GH(\gamma f_0)=a_\gamma \quad (\gamma=0,\pm 1,...), \quad (19)$$

$$GH(\gamma f_0)=\frac{1}{T}\sum_{m=-\infty}^{\infty} G[(\gamma+mN)f_0]. \quad (20)$$

So,

$$Ta_\gamma=\sum_{m=-\infty}^{\infty} G[(\gamma+mN)f_0]. \quad (21)$$

Substitute Ta_γ into (17) we finally get:

$$G_d(\gamma f_0)=\sum_{m=-\infty}^{\infty} G[(\gamma+mN)f_0]. \quad (22)$$

By considering the scaling factor T in (20) we can find $G_d(\gamma f_0)$ or $GH(\gamma f_0)$ is the final result we get according to the numerical integration and the DFS respectively. It is not the field of the observation point in the γth cell we wanted, but a superposition of the field at a set of periodic observation points with period Nf_0, which can be shown in Fig. 1 along z direction in space domain with the consideration of $f_0 = \alpha$. The mark ○ denote the observation points at positive z direction and ◎ denote the points at negative direction if the source is set at the origin, where reveals the aliasing problem clearly in the ASM-FDTD.

Suppose the velocity of propagation is v_0, convert (22) into time domain we obtain:

$$G_d(|\gamma| f_0/v_0) = \sum_{m=-\infty}^{\infty} G[|(\gamma + mN)| f_0/v_0]. \quad (23)$$

(23) can be shown by Fig. 2, here the mark ○ and ◎ denote the points in time domain corresponded to the observation points' position in Fig. 1, they are symmetric with each other at the points of $|mN\alpha|/(2v_0)$.

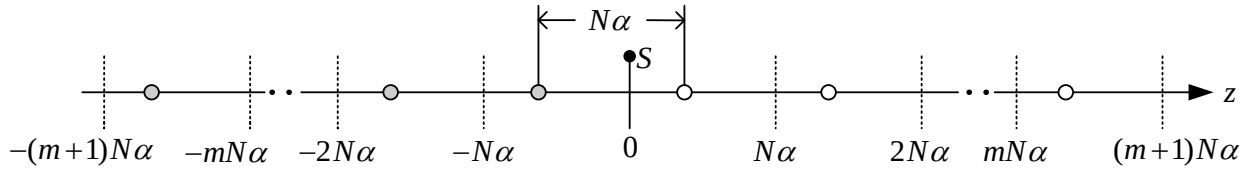

Fig. 1. Aliasing problem in space domain.

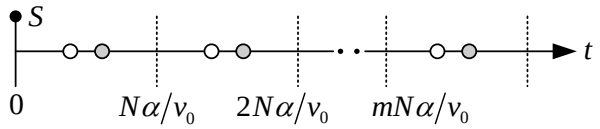

Fig. 2. Aliasing problem in time domain

To lessen the aliasing problem, the interval of the points in time domain shown in Fig. 2 should be apart from each other as much as possible, it can be achieved by increasing N or enlarging α, both of them will heavily increase the computational requirements. The effective interval T_d is its least distant to the adjacent points. From (23) and Fig. 2, any sampling point at cell γ except $\gamma \le N/2$, the T_d can be shown as:

$$T_d = \min[2\,\mathrm{mod}(\gamma, N/2), N - 2\,\mathrm{mod}(\gamma, N/2)]\alpha/v_0. \quad (24)$$

We will get $T_{d\max} = N\alpha/(2v_0)$ when set the sampling points at $\gamma = (2m+1)N/4$. A further analysis shows that the two symmetric points overlap with each other when $\gamma = mN/2$, if the periodic cell is symmetric itself and both r_0 and r are at symmetric position, the field of the two symmetrical sampling points will be exactly equal, then the output of ASM-FDTD will be accurately double to the standard FDTD method, the effective interval will be $T_d = N\alpha/v_0$, and a minimum aliasing error will appear. But if $G(nf_0)$ is infinite duration in time domain, the period of $N\alpha$ should tend to infinite to avoid the aliasing problem and there will be no advantage of ASM-FDTD.

III. PRONY'S METHOD ANALYSIS AND EXTRAPOLATION

We now outline the Prony's method to fit the deterministic exponential model to the integral field $E_{tot}^{\infty}(r, r_0, k_z, t)$ in (2) with respect to every spectral sampling points k_z, which can be concisely expressed as the form:

$$\hat{E}_{tot}^{\infty}(r, r_0, k_z, t) = \sum_{m=1}^{M} h_m(k_z) e^{s_m(k_z)t}, \quad (25)$$

both $h_m(k_z)$ and $s_m(k_z)$ are complex here. The structure of the tunnel in the ASM-FDTD is periodic in the z direction shown in Fig. 3. The top curved interface is dealt with Conformal FDTD (CFDTD) [20], outside of the soil is truncated by convolution PML (CPML) [21] and the infinite periodic structure is truncated in the z direction with the PBC.

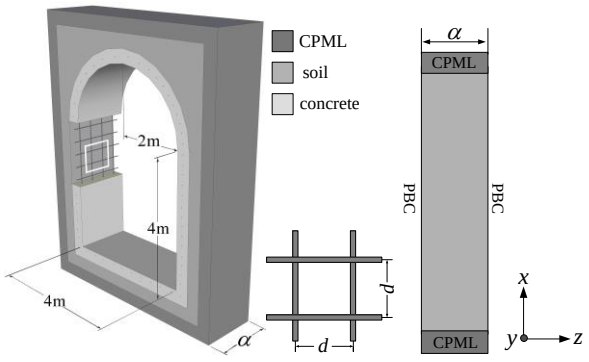

Fig. 3. Geometry of the periodic tunnel structure.

The parameters for the soil are dielectric constant $\varepsilon_r = 10.0$ and conductivity $\delta = 1.0e-3\text{s/m}$. For the concrete $\varepsilon_{rc} = 6.0$ and $\delta_c = 5.0e-4\text{s/m}$ with the thickness $w = 0.2666\text{m}$, the interval of the steel bar contained in the middle of concrete is $d = 0.1333\text{m}$, the top vaulted part is a semicircle with the radius $r = 2.0\text{m}$.

In the waveguide system [22], the excitation source is usually introduced robustly according to the propagation model such as TE10 and TM11. Though in this case we can't get the analytical model of the wave propagation, the way that the excitation sources induced in the waveguide system can still be employed here. It can be shown as:

$$E_{tan}^{n+1}(i,j,k_s) = E_{tan}^{n}(i,j,k_s) + f(i,j,k_s)g(t), \quad (26)$$

the subscript 'tan' denotes the E-field distributed in a transverse cross section at $z = k_s \Delta z$ of the tunnel structure in Fig. 3, $f(i,j,k_s)$ is the function of the field distribution and $g(t)$ refers to the time function determine the bandwidth of the sources. Here we set $f(i,j,k_s)$ as the model of TE10 in waveguide with the size of $a \times b = 4.0\text{m} \times 6.0\text{m}$. Though the model doesn't satisfy the boundary condition of the tunnel, we can consider that after some length propagation the model will be in a steady state which approach TE10 propagation model of the tunnel itself.

In ASM-FDTD the spectral points are sampled as the midpoint rule of integration that:

$$k_z = \xi_i = \frac{\pi}{\alpha}[-1 + \frac{2i-1}{N}], \quad (27)$$

the number of sampling points $N = 80$, for the property (7) of ASM-FDTD we compute the $E_{tot}^{\infty}(r, r_0, k_z, t)$ with respect to $\xi_i < 0$, period of the single cell $\alpha = 0.4\text{m}$, $g(t)$ in (26) set to be a differential Gaussian electric pulse that $g(t) = E_0(t - t_0)\exp(4\pi(t-t_0)^2/\tau^2)$ with $\tau = 3.0\text{ns}$, $E_0 = 1000\,\text{V/m}$ and $t_0 = 2\tau$, $f(i,j,k_s)$ located at the $x-y$ plane with $z = \alpha/2$, Yee cell size is given by $\Delta x = \Delta y = \Delta z = 0.01333\text{m}$ and the time step is $\Delta t = 22.16\text{ps}$. The simulation is performed for 40000 time steps and a probe is placed at $(a/2, b/2, \alpha/2)$ to sample the y-component of the E-field.

In the Prony's method with respect to every spectral sampling point k_z in Brillouin zone, we set the model order $M = 18$, the analyzed data sampled since the 10000th time step to ensure the propagation model to settle down, the samples between 10000 to 15000 are used for estimating the exponential models, and the rest are used for prediction comparison, the sampling interval is 22 time steps that 227 modeling samples are obtained. Figures 4 (a) and (b) show the comparisons of the extrapolation results based on the exponential models to the original result of TD field $E_{tot}^{\infty}(r, r_0, k_z, t)$ in ASM-FDTD for $\xi_i \alpha/\pi = -0.7625$ and $\xi_i \alpha/\pi = -0.2625$ in (27) respectively, from which we can find that they are in good agreement. It can be seen that in the implementation of the ASM-FDTD to simulate the EMP propagation in the periodic tunnel structure, the total field $E_{tot}^{\infty}(r, r_0, k_z, t)$ can be expressed as a linear superposition of complex exponentials with high accuracy, so we just determine the models of exponential from a finite early-time response, the later time response can be obtained by extrapolation from the exponential models. In this case, if the simulation had been stopped at 15000 time steps instead of the 40000 time steps, saving about 63% in terms of simulation time will be obtained, and this percentage would be much greater as the simulation time steps increase.

To further verify the accuracy of the exponential models, in (13) we set $n = 50$, Fig. 5 shows a comparison between the final numerical integration results obtained based on the exponential models and the ASM-FDTD method. From the figure, we can see they agree well with each other. And we find the aliasing problem in ASM-FDTD apparently, with a further analysis from Fig. 2 we know that the main waveform in the figure consist of the field at the probes of $(\gamma = 50, m = 5)$ and $(\gamma = 50, m = -6)$ in (22), which are 180m and -172m far away off the excitation source along the *z* direction respectively.

In equation (25), $h_m(k_z)$ and $s_m(k_z)$ can be defined as:

$$\begin{aligned} h_m(k_z) &= A_m(k_z)\exp(j\theta_m(k_z)) \\ s_m(k_z) &= \sigma_m(k_z) + j\omega_m(k_z) \end{aligned}, \quad (28)$$

A_m is the amplitude of the complex exponential, θ_m is the initial phase in radians, σ_m is the damping factor, and ω_m is the frequency. The model order $M = 18$, for concisely expressed we select two representative terms, Fig. 6 shows the parameters versus to the sampling spectral points corresponding to the order $m = 1$ and $m = 2$. In fact for the analyzed data is real, the complex exponentials must occur in complex conjugate pairs of equal amplitude, so the $M/2$ terms of the orders are significant. We can see the parameter $\omega_m(k_z)$ presents a very well continuous linear character, $A_m(k_z)$ and $\sigma_m(k_z)$ changes with different orders. Some discontinuous appear in those curves just at the points with the amplitude is low or the damping factor is high. For the parameter $\theta_m(k_z)$, it is so oscillatory of some orders even when the amplitude values are great.

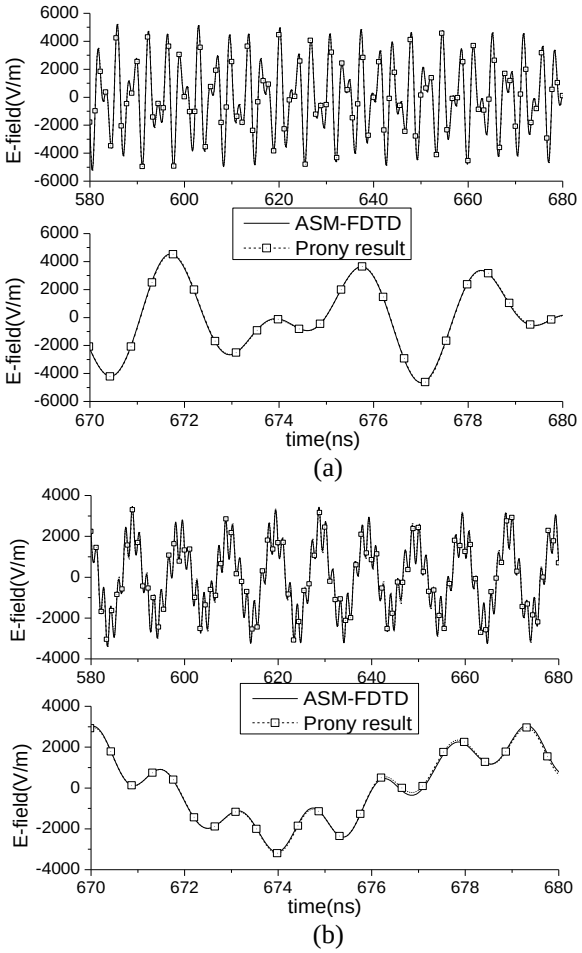

Fig. 4. Comparison of the integral field in ASM-FDTD and the exponential model result for: (a) $\xi_i \alpha/\pi = -0.7625$ and (b) $\xi_i \alpha/\pi = -0.2625$.

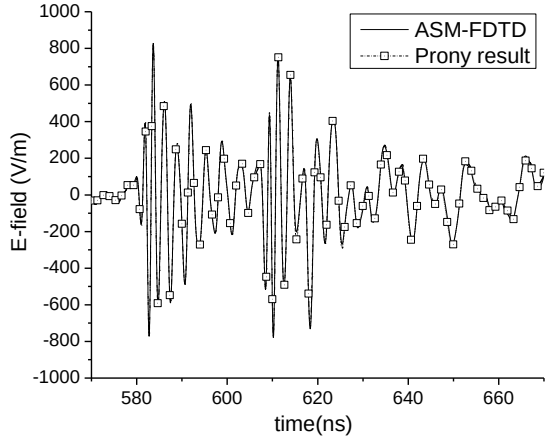

Fig. 5. Comparison of the $E_{tot}(r + n\alpha 1_z, r_0, t)$ computed from the original time response and extrapolated time response with the exponential models.

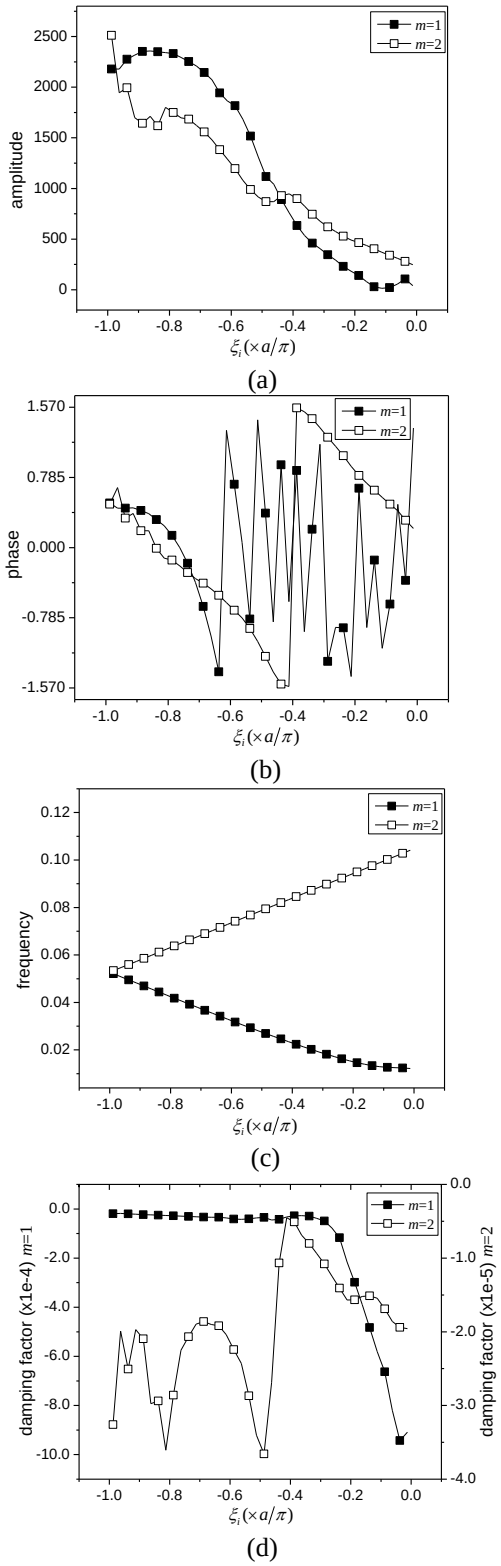

Fig. 6. Parameters of the exponential models versus the sampling spectral points in Brillouin zone, for expressing concisely here we set $\Delta t = 1$.

IV. ALIASING PROBLEM SOLVED BY INTERPOLATION

The aliasing problem in ASM-FDTD can be overcome by increasing the number of spectral sampling points with the cost of computational requirement. In Section III, we find that the integral field correspond to the sampling points can be represented by sums of damped exponentials, so if we obtain the parameters of the exponentials at every spectral points, the aliasing problem can then be solved. In this section we will estimate the parameters through interpolation, and then solve the aliasing problem in the ASM-FDTD. Cubic spline interpolation is employed here for its smooth graph and continuously turning tangent.

Figure 6 show the parameters of the exponential models versus the sampling spectral points, one point should be emphasized here is the parameter of phase, which is obtained by the function of inverse tangent. Correspond to the order $m=2$ we can obtain a smoother phase plots by unwrapping, but to the order of $m=1$ there are too many discontinuities that we can't set a correct jump tolerance to get the right unwrapped result. Furthermore the phase θ_m in (28) is at the range of $[-\pi,\pi]$, but the phase we get by inverse tangent is at $[-\pi/2,\pi/2]$, so it needs to combine other information such as the phase obtained by inverse cosine or sine to convert the phase from the range of $[-\pi/2,\pi/2]$ to the range of $[-\pi,\pi]$. So, we transform the equation in (28) to:

$$h_m(k_z) = p(k_z) + jq(k_z), \tag{29}$$

which can avoid the above problem properly. The parameters $p(k_x)$ and $q(k_z)$ corresponding to the order $m=1$ and $m=2$ are shown in Fig. 7.

Set the endpoint condition of the interpolation to be:

$$\begin{aligned} \rho_0 &= \rho_1 \\ \rho_{M+1} &= \rho_M \end{aligned}. \tag{30}$$

Take the imaginary part of the amplitude as example, the resulting curve of interpolation is shown in Fig. 8. The other parameters have the same smooth results as the figure shown.

Based on the above analysis, a probe is set at $(a/2,b/2,l_z/2)$, according to the conclusion in Section II, we can set the number of sampling points:

$$N_{interp} = \frac{4(l-l_0)}{\alpha} \quad (l > l_0). \tag{31}$$

The first waveform of $n = N_{interp}/4$ in (13) is the transient field we want. Of course we can also set other algorithm according (23) just ensure $n\alpha = l - l_0$ and the effective interval in (24) is broad enough.

Figure 5 shows the aliasing results consist of the field with probes of 180m and -172m distant to the excitation sources, follow the above criterions we set $N_{interp} = 360$ and $n = 90$. Figure 9 shows the comparison between the picked-up result and the MW-FDTD method where the length of window to be set 20m to lessen the truncation error. As seen from the figures, these results are consistent well to each other.

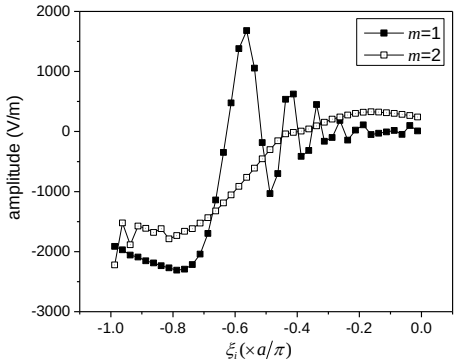

(a)

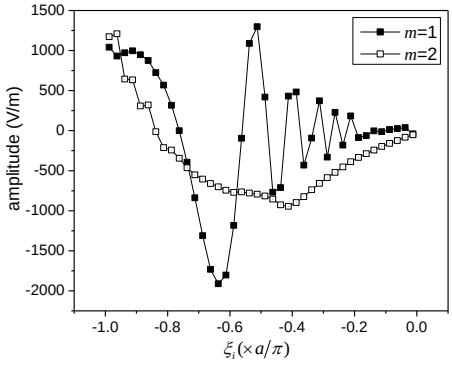

(b)

Fig. 7. Parameter of the complex amplitude versus the sampling spectral points in Brillouin zone: (a) the real part and (b) the imaginary part.

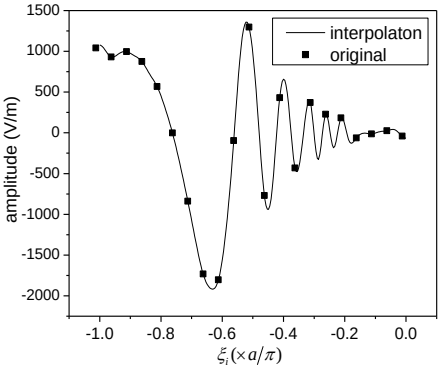

Fig. 8. The cubic spline interpolation result based on the imaginary part of the amplitude.

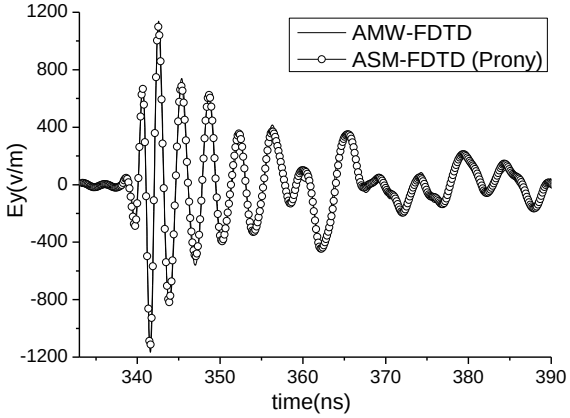

Fig. 9. Comparison of picked-up result from the aliasing output of ASM-FDTD with the MW-FDTD result.

V. CONCLUSION

In this paper, the aliasing problem in the ASM-FDTD has been presented in detail. To overcome the problem, the Prony's method is employed to fit an exponential model with the total field of ASM-FDTD and a good agreement is observed. By extrapolating the total field based on the exponential model and interpolating the exponential parameters correspond to the spectral points in Brillouin zone, the computational requirement is drastically reduced and the aliasing problem is solved. Results show good agreement with the MW-FDTD. This method can also be applied to deal with the aliasing problem in the implementation of the ASM-FDTD to simulate some other periodic structures, and some other interpolation methods and curve-fitting approximation [23] maybe more appropriate for this problem.

ACKNOWLEDGMENT

This work was supported by Chinese National Science Foundation under Grant No. 60971063.

REFERENCES

[1] D. G. Dudley, M. Lienar, S. F. Mahmud, and P. Degauque, "Wireless propagation in tunnels," *IEEE Antennas Propag. Magazine*, vol. 49, pp. 11-26, 2007.

[2] Y. P. Zhang, "Novel model for propagation loss prediction in tunnels," *IEEE Trans. Veh. Technol.*, vol. 52, pp. 1308-1314, 2003.

[3] E. Heyman, R. Kastner, and R. W. Ziolkowski, "Hybrid Ray-FDTD moving window approach to pulse propagation," *Journal of Computational Physics*, vol. 138, pp. 480-500, 1997.

[4] J. F. Liu, X. L. Xi, G. B. Wan, and L. L. Wang, "Simulation of electromagnetic wave propagation through plasma sheath using the moving window finite-difference time-domain method," *IEEE Trans. on Plasma Science*, vol. 39, pp. 852-855, 2011.

[5] G. S. Ching, M. Ghoraishi, M. Landmann, and H. Sakamoto, "Wideband polarimetric directional propagation channel analysis inside an arched tunnel," *IEEE Trans. Antennas Propagat*., vol. 57, pp. 760-767, 2009.

[6] K. Guan, Z. Zhong, B. Ai, and C. Briso-Rodriguez, "Complete propagation model in tunnels," *IEEE Antennas and Wireless Propagation Letters*, vol. 12, pp. 741-743, 2013.

[7] K. S. Yee, "Numerical solution of initial boundary value problems involving Maxwell's equations in isotropic media," *IEEE Trans. Antennas Propagat.*, vol. 14, pp. 302-307, 1966.

[8] A. Taflove and S. C. Hagness, *Computational Electrodynamics: The Finite-Difference Time-Domain Method*. 2nd ed., Boston, MA: Artech House, 2000.

[9] J. W. Schuster, K. C. Wu, R. R. Ohs, and R. J. Luebbers, "Application of moving window FDTD to predicting path loss over forest covered irregular terrain," *Antennas and Propagation Society International Symposium*, pp. 1607-1610, 2004.

[10] Y. Wu and I. Wassell, "Introduction to the segmented finite-difference time-domain method," *IEEE Trans. on Magnetics*, vol. 45, pp. 1364-1367, 2009.

[11] M. M. Rana and A. S. Mohan, "Segmented locally one dimensional FDTD method for EM propa-gation inside large complex tunnel environments," *IEEE Trans. on Magnetics*, vol. 48, pp. 223-226, 2012.

[12] F. Akleman and L. Sevgi, "Realistic surface modeling for a Finite Difference Time Domain wave propagator," *IEEE Trans Antennas Propagat.*, vol. 51, no.7, July 2003.

[13] Y. Xiaoshuan and B. Chen, "Application of MW-FDTD to simulate the electromagnetic pulse (EMP) propagation in tunnel, *CEEM'2009*, pp. 200-203, 2009.

[14] R. Qiang, J. Chen, F. Caploino, and D. R. Jackson, "ASM-FDTD: A technique for calculating the field of a finite source in the presence of an infinite periodic artificial material," *IEEE Microw. Wireless Compon. Lett.*, vol. 17, no. 4, Apr. 2007.

[15] R. Qiang, J. Chen, and F, Yang, "FDTD simulation of infrared FSS transmission spectrum from oblique incidence," in Proc. *IEEE Antennas Propag. Soc. Int. Symp*., pp. 2715-2718, June 2006.

[16] B. A. Munk and G. A. Burrel, "Plane-wave expansion for arrays of arbitrarily oriented piecewise linear elements and its application in

determining the impedance of a single linear antenna in a lossy half-space," *IEEE Trans. Antennas Propag*., vol. AP-27, no. 5, pp. 331-343, May 1979.

[17] A. Aminian and Y. Rahmat-Sammii, "Spectral FDTD: A novel technique for the analysis of oblique incident plane wave on periodic structures," *IEEE Trans. Antennas Propag.*, vol. 54, no. 6, pp. 1818-1825, June 2006.

[18] S. L. Marple, *Digital Spectral Analysis with Applications*. Englewood Cliffs, NJ: Prentice-Hall, Inc., Ch. 11, 1987.

[19] E. O. Brigham, *The Fast Fourier Transform*. Englewood Cliffs, NJ: Prentice-Hall, Inc., Ch. 5-6, 1974.

[20] W. Yu and R. Mittra, "A conformal finite difference time domain technique for modeling curved dielectric surfaces," *IEEE Microw. and Wireless Compon. Lett.*, vol. 11, no. 1, Jan. 2001.

[21] J. Alan Roden and S. D. Gedney, "Convolution PML: An efficient FDTD implementation of the CPF-CPML for arbitrary media," *Microw. and Optl. Technol. Lett.*, vol. 27, no. 5, Dec. 5, 2000.

[22] A. Taflove, *Computational Electrodynamics: The Finte-Difference Time-Domain Method*. Boston, MA: Artech House, Ch. 5, 1995.

[23] A. K. Shaw, "Optimal identification of discrete-time systems from impulse response data," *IEEE Trans Signal Processing*, vol. 42, no. 1, Jan. 1994.

Yun-Fei Mao was born in Zhejiang Province, China, in 1984. He received the B.S. degrees, the M.S. degree and the Ph.D. degree in Electric systems from Nanjing Engineering Institute, Nanjing, China, in 2006, 2009 and 2013 respectively. He is currently working in China Satellite Maritime Tracking and Control Department, Yuan Wang III, Jiangyin 214400, China. His research interests include computational electromagnetic and electro-magnetic tracking.

Hong-Bing Wu was born in Jiangsu Province, China, in 1987. He is currently working in China Satellite Maritime Tracking and Control Department, Jiangyin 214400, China. His research interests include inertial navigation and electromagnetic tracking.

Jia-Hong Chen was born in Jiangsu, China, in 1969. He received the B.S. and M.S. degrees in National University of Defense Technology, Changsha, China, in 1982 and 1987, respectively, and the Ph.D. degree in Control Engineering from Xi'an Jiao Tong University, Xi'an, China. His research interests include electromagnetics and electromagnetic tracking.

Xu-Wei Su was born in Hubei Province, China, in 1983. He received the B.S. in Xidian University, Xi'an, China, in 2001. He is currently working in China Satellite Maritime Tracking and Control Department, Jiangyin 214400, China. His research interests include electromagnetics and electromagnetic tracking.